Tectonophysics, 211 (1992) 23–43
Elsevier Science Publishers B.V., Amsterdam

Influence of asperities along subduction interfaces on the stressing and seismicity of adjacent areas

R. Dmowska [a,b] and L.C. Lovison [b]

[a] *Division of Applied Sciences, Harvard University, Cambridge, MA 02138, USA*
[b] *Department of Earth and Planetary Sciences, Harvard University, Cambridge, MA 02138, USA*

(Received March 14, 1991; revised version accepted December 4, 1991)

ABSTRACT

Dmowska, R. and Lovison, L.C., 1992. Influence of asperities along subduction interfaces on the stressing and seismicity of adjacent areas. In: T. Mikumo, K. Aki, M. Ohnaka, L.J. Ruff and P.K.P. Spudich (Editors), Earthquake Source Physics and Earthquake Precursors. *Tectonophysics*, 211: 23–43.

We have investigated the influence of large-scale fault inhomogeneities in large subduction earthquakes on the style of deformation and seismic behavior of the incoming oceanic plate and slab at intermediate depths during the earthquake cycle. The zones of the large subduction events of Rat Islands 1965, Alaska 1964 and Valparaiso 1985 have been searched for earthquakes with $m_b \geqslant 5.0$, if available, and for time periods as long as possible. It has been found that in general the seismicity in the incoming oceanic plate clusters in front of asperities (= areas of highest seismic moment release and strongest locking) and is positioned relative to them in the direction of plate motion. It is usually lacking in areas adjacent to non-asperities, that is to zones that slip during the main event but with appreciably smaller seismic moment release, and possibly slip seismically/aseismically during the whole cycle. Similar behavior occurs in the downgoing slab at intermediate depths, where seismicity during the cycle clusters (but less strongly than in the oceanic crust) next to asperities and down-dip from them. We infer that the locking of asperities causes higher stresses associated with the earthquake cycle itself to occur in areas adjacent to asperities, both up-dip and down-dip from them along the direction of plate motion, and that such stressing is much less pronounced in the areas adjacent to non-asperities. This opens the possibility of identifying the areas of highest seismic moment release in future subduction earthquakes, and carries implications for where the highest deformation and, possibly, precursory phenomena and/or nucleation of a future event might occur.

Introduction

Recent observational and theoretical work on earthquake cycles in subduction zones (Christensen and Ruff, 1983, 1988; Dmowska et al., 1988; Dmowska and Lovison, 1988; Astiz et al., 1988; Lay et al., 1989) has explained certain seismic phenomena in relation to stress accumulation and release associated with great underthrust events. It has been realized that temporal variations of stress, associated with earthquake cycles, occur in the subducting slab and, as well, in the area of the outer-rise, oceanward from the main zones of subduction earthquakes. In the outer-rise, the bending stresses present get overprinted with tensional stresses in the beginning of the cycle, caused by the slip in the main subduction event. By the latter, part of the cycle that has changed to a compressional overprint, occurring because the main thrust zone remains locked while converging motion of the remote ocean floor continues. These factors result in typical tensional outer-rise earthquakes following large subduction events, as well as sporadic compressional ones preceding large subduction events, as documented in the works cited above.

At intermediate depths, in the down-going subducting slab, the tensional stresses caused by slab pull receive a superposed compressional component in the beginning of the cycle, caused

Correspondence to: R. Dmowska, Division of Applied Sciences, Harvard University, Cambridge, MA 02138, USA.

by the slip in the main thrust subduction event. In the latter part of the cycle the continuing slab pull and the locking of main thrust zone result in higher tensional stresses at intermediate depths.

We have combined the recent insights just summarized with the results of studies of spatial and temporal heterogeneities of seismic moment release in some large subduction events by Ruff (1983), Ruff and Kanamori (1983), Beck and Ruff (1984), Schwartz and Ruff (1985, 1987), Christensen and Ruff (1986), Kikuchi and Fukao (1987), Beck and Ruff (1987), and Beck and Christensen (1991). In those works, body wave inversion techniques and studies of directivity of the rupture process reveal the spatial distribution of the areas of highest seismic moment release (or highest slip), such areas being called "asperities". Some of the methods used allow for placement of the most pronounced asperities only, and basically only along the strike of the rupture zone; the extent of asperities along the dip could not be assessed. Other methods (e.g., Kikuchi and Fukao, 1985, 1987) place asperities of different sizes both along the strike of the aftershock zone and along the width. Collections of smaller asperities could be then interpreted as larger ones defined by other methods. By now a few large subduction events have been analyzed in this way, including Alaska 1964, Kuriles 1963, Colombia 1979, Valparaiso 1985, Rat Islands 1965, Tokachi-Oki 1968, Kurile Islands 1969, and Andreanof Islands 1986. Knowledge of the spatial distribution of seismic moment release is of importance not only from the point of view of basic understanding of the earthquake rupture process, but also for purposes of seismic hazard assessment, if we assume that whatever the mechanical causes of a particular asperity distribution, they would act again in the same places in a future large earthquake. These distributions have important implications for engineering seismology, as shown by recent work on simulations of strong ground motions based on known distributions of seismic moment release in the plane of rupture (Somerville et al., 1991), and on comparisons of strong ground motion spectra with teleseismic spectra (Houston and Kanamori, 1990). Recent attempts to understand the relationship between seismicity in the area of the rupture zone itself and moment release in the great earthquake (Mendoza and Hartzell, 1988; Choy and Dewey, 1988; Houston and Engdahl, 1989; Schwartz et al., 1989; Engdahl et al., 1989; Hartzell and Iida, 1990; Oppenheimer et al., 1990) suggest that none or few preshocks or aftershocks occur in regions of the main asperities. This would suggest in turn that asperities are zones locked between main earthquakes, while other areas within the thrust interface slip aseismically or exhibit lower-magnitude seismicity (and/or rupture in aftershocks after the main event).

If this is true, it should be possible to identify the locations of the largest asperities in zones of large subduction earthquakes through the use of seismicity distributions in the outer-rise zones adjacent to mainshock rupture planes, and intermediate-depth seismicity as well. That is because the pulsating stresses associated with the earthquake cycle of the main subduction event should have a higher magnitude in the outer-rise and down-dip areas adjacent to an asperity than in areas adjacent to zones with lower moment release in the mainshock. The latter have lower slip during the mainshock and must slip aseismically and/or with moderate seismicity during the cycle, and hence do not generate nearby stress fluctuations, associated with stress accumulation and release in the earthquake cycle, as effectively as the more strongly locked asperities. Thus the large compressional earthquakes in the outer-rise in the latter part of an earthquake cycle, if at all present, should occur preferentially in the areas adjacent to zones of future higher moment release (asperities). Also, the tensional earthquakes in the outer-rise, following the main subduction event, should concentrate in areas neighboring asperities. The same should be true for the seismicity at intermediate depth, that is the effects of locking of asperities should be more pronounced adjacent to asperities. That is, the higher tensional seismicity in the down-going slab towards the end of the cycle should concentrate close to asperities, especially at shallow depths (40–100 km). This should allow the use of outer-rise and intermediate-depth seismicity to identify the future areas of highest moment release, e.g., in

zones where the previous large subduction event occurred long enough in the past (before 1960 or so) that data quality does not allow asperities to be identified from its seismic radiation.

The purpose of the present work is to check such a hypothesis, and we achieve it by analysis of seismicity associated with some earthquakes with known large asperities: Rat Islands 1965, Alaska 1964 and Valparaiso 1985. The areas are searched for earthquakes with $m_b \geq 5.0$ if available, and for as long time periods as possible, in the regions of the outer-rise and in the downgoing slab adjacent to the zones of main ruptures.

Rat Islands earthquake of February 4, 1965

The great Rat Islands earthquake of Feb. 4, 1965 ($M_w = 8.7$) ruptured a 650-km-long segment of the obliquely convergent boundary between the Pacific and North American plates, along the western end of the Aleutian Islands (Fig. 1). To the east, the segment abuts on the strip that ruptured in the great 1957 Aleutian earthquake ($M_w = 9.1$). To the northwest, the plate movement along the southern side of the Commander Islands is almost parallel to the plate boundary and occurs along shallow-dipping thrust faults (Cormier, 1975); the area was a site of two large earthquakes in 1849 and 1858 and is currently a gap. The average velocity of plate motion, calculated at 178°E and 51°N, based on the Minster and Jordan (1978) model, is about 8 cm/yr at 310° (shown as an arrow in Fig. 1), though the subduction rate normal to the arc is only around 5 cm/yr in that place, and diminishes to zero westward along the arc.

The aftershock zone shown in Figure 1 is based on the relocations of aftershocks with $m_b \geq 5.3$ performed by Spence (1977), for events occurring between the main earthquake and March 30, 1965 and having 70 or more teleseismic P-wave observations. P-wave arrival times from the nuclear explosion Long Shot and from an event on Sept. 27, 1965 were the reference data for the relocation. The relocated aftershocks define an area around 650 km long and 50–60 km wide.

The hatched areas in Figure 1 are the areas of highest seismic moment release, interpreted as

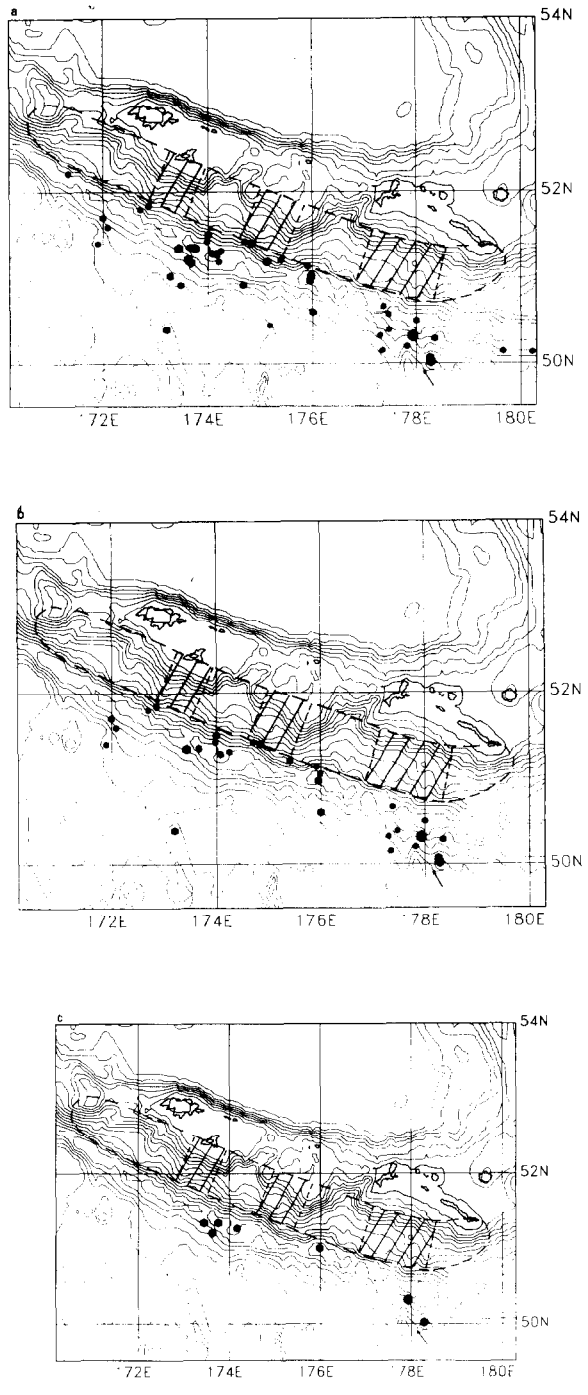

Fig. 1. The aftershock zone (dotted line) of the February 4, 1965 Rat Islands earthquake in the western Aleutians with three areas of highest seismic moment release (hatched, after Beck and Christensen, 1991). Black symbols denote epicenters of pre-trench and outer-rise earthquakes for the period Feb. 4, 1965 to Aug. 31, 1987: (a) for all events with $m_b \geq 5.0$, (b) for events with $m_b \geq 5.0$ during the first year after the mainshock, (c) for all events with $m_b \geq 5.7$. Size of black symbol is proportional to earthquake magnitude.

TABLE 1

Rat Islands earthquake of February 4, 1965

Date	Lat. (°N)	Long. (°E)	Depth (km)	m_b	M_s	F.M.	Ref.
Outer-rise earthquakes:							
Feb. 4, 1965	50.40	173.20	35	5.5			R
Feb. 4, 1965	51.40	174.84	33	5.5			R
Feb. 4, 1965	51.50	174.00	33	5.4			R
Feb. 4, 1965	51.84	172.86	33	5.2			R
Feb. 4, 1965	51.40	171.90	33	5.0			R
Feb. 4, 1965	51.42	174.71	35	5.1			R
Feb. 4, 1965	51.80	172.70	0	5.0			R
Feb. 5, 1965	50.60	176.00	25	5.5			R
Feb. 5, 1965	51.20	175.40	34	5.2			R
Feb. 6, 1965	51.28	174.07	61	5.3			R
Feb. 7, 1965	51.13	175.91	40	5.2			ISC
Feb. 7, 1965	51.34	173.44	45	5.8		T	ISC/CR
Feb. 11, 1965	51.04	175.98	78	5.0			ISC
Mar. 5, 1965	51.70	172.00	33	5.3			ISC
Mar. 15, 1965	51.31	174.25	33	5.1			ISC
Mar. 30, 1965	50.32	177.93	20	6.5	7.5	T	ISC/CR
Mar. 30, 1965	50.20	177.82	33	5.1			ISC
Mar. 30, 1965	50.33	177.30	33	5.0			ISC
Mar. 30, 1965	50.50	178.00	30	5.0			ISC
Mar. 30, 1965	50.15	177.34	33	5.1			ISC
Mar. 31, 1965	50.39	177.47	24	5.0			ISC
Mar. 31, 1965	50.29	178.35	48	5.3			ISC
Apr. 13, 1965	50.66	177.37	35	5.0			ISC
Apr. 13, 1965	51.59	172.09	5	5.1			ISC
May 20, 1965	51.35	173.67	41	5.2			ISC
June 15, 1965	50.07	178.26	26	5.4			ISC
July 22, 1965	50.96	175.95	44	5.3			ISC
Oct., 1, 1965	50.02	178.28	5	6.2		T	ISC/CR
Nov. 11, 1965	51.42	173.98	45	5.0			ISC
June 2, 1966	51.01	175.98	48	5.7		T	ISC/CR
Oct. 25, 1968	50.57	177.46	23	5.0			ISC
Apr. 4, 1969	51.17	173.67	35	5.6			ISC
Feb. 27, 1970	50.13	180.22	21	5.0			ISC
Mar. 19, 1970	51.34	173.75	8	5.8	6.2	T	ISC/CR
July 24, 1970	52.23	171.34	48	5.0			ISC
Mar. 23, 1973	51.27	174.16	21	5.7			ISC
Aug. 18, 1974	50.45	175.18	32	5.0			ISC
Aug. 10, 1975	51.18	174.21	17	5.0			ISC
Oct. 17, 1976	50.14	179.66	29	5.1			ISC
Aug. 18, 1977	50.91	174.68	32	5.3			ISC
July 20, 1978	51.19	175.15	54	5.2	4.8	S	ISC/HAR
Oct. 4, 1978	50.91	173.48	36	5.3	5.0	T	ISC/HAR
Jan. 22, 1979	51.18	175.13	52	5.4	4.6	S	ISC/HAR
May 3, 1980	51.21	173.62	38	5.8	5.3	T	ISC/HAR
Jan. 31, 1985	51.35	173.64	44	5.0			ISC
Apr. 9, 1986	51.02	173.28	15	5.4	4.7	T	ISC/HAR
Intermediate-depth earthquakes:							
July 14, 1940	51.75	177.50	80		7.4 +		GR49
Sept. 16, 1950	52.00	177.10	100	6.5		C	FK81
Apr. 29, 1963	51.30	178.70	56	5.9			USGS
Apr. 30, 1963	51.20	178.60	60	5.4			USGS

TABLE 1 (continued)

Date	Lat. (°N)	Long. (°E)	Depth (km)	m_b	M_s	F.M.	Ref.
Apr. 30, 1963	51.30	178.60	45	5.8			USGS
Jan. 3, 1964	52.90	173.16	90	5.0			ISC
Feb. 8, 1964	52.25	175.52	43	5.4			ISC
Aug. 17, 1964	51.50	177.70	74	5.2			ISC
Jan. 30, 1965	51.68	179.67	88	5.1			ISC
Feb. 5, 1965	51.80	176.70	74	5.1			ISC
Feb. 5, 1965	52.20	175.10	42	5.1			ISC
Feb. 9, 1965	52.27	179.64	40	5.1			ISC
Feb. 18, 1965	51.45	179.28	48	5.6			ISC
Feb. 23, 1965	52.69	173.04	51	5.0			ISC
Mar. 4, 1965	52.04	175.14	57	5.3			ISC
Mar. 7, 1965	51.85	176.42	47	5.2			ISC
June 3, 1965	51.91	175.83	46	5.3			ISC
July 2, 1965	52.03	175.47	45	5.2			ISC
Feb. 27, 1966	52.19	175.06	48	5.0			ISC
July 4, 1966	51.78	176.44	41	5.5			ISC
Aug. 1, 1966	51.65	177.70	46	5.1			ISC
Aug. 18, 1966	51.62	177.91	43	5.2			ISC
Sept. 8, 1966	52.76	173.43	63	5.0			ISC
Nov. 14, 1967	51.90	178.06	122	5.2			ISC
Feb. 26, 1968	52.67	172.47	44	5.1			ISC
Mar. 11, 1968	52.05	178.25	141	5.0			ISC
July 3, 1969	51.76	178.04	86	5.1			ISC
Sept. 15, 1969	51.87	175.47	42	5.4			ISC
Feb. 18, 1970	52.12	175.48	51	5.0			ISC
Apr. 29, 1970	51.72	177.03	52	5.1			ISC
Apr. 30, 1971	51.66	179.91	95	5.2			ISC
Nov. 30, 1971	51.09	179.70	63	5.0			ISC
Dec. 6, 1971	52.22	179.68	169	5.0			ISC
Dec. 8, 1971	51.69	178.44	82	5.2			ISC
Feb. 1, 1972	51.75	177.72	70	5.1			ISC
June 19, 1972	52.14	175.09	46	5.3			ISC
Nov. 21, 1972	52.44	173.57	42	5.5			ISC
Jan. 13, 1973	51.78	176.27	43	5.0			ISC
Feb. 1, 1973	51.70	176.26	43	5.3			ISC
Mar. 19, 1973	52.78	173.85	81	5.7		C	ISC/WT
June 17, 1973	51.75	176.35	42	5.0			ISC
Nov. 9, 1973	52.42	178.36	183	5.5			ISC
June 15, 1974	52.23	178.86	160	5.5			ISC
Aug. 20, 1974	52.17	174.95	42	5.7			ISC
Apr. 30, 1975	51.35	179.70	49	5.2			ISC
June 15, 1975	51.59	179.53	73	5.0			ISC
Nov. 6, 1975	51.79	176.21	43	5.4			ISC
Aug. 23, 1978	51.70	176.40	46	5.4	5.0	C	ISC/HAR
Nov. 3, 1978	51.96	174.92	42	5.0	5.1		ISC
Oct. 18, 1979	51.82	177.12	60	6.0		S	ISC/HAR
June 12, 1980	51.65	177.68	63	5.0			ISC
Feb. 27, 1981	51.77	176.32	46	5.2	4.0		ISC
Apr. 30, 1982	51.60	176.75	59	5.0			ISC
Dec. 24, 1982	52.60	173.17	62	5.2			ISC
Apr. 3, 1983	51.97	179.25	116	5.6		S–C	ISC/HAR
Mar. 30, 1984	51.32	177.95	57	5.0			ISC
May 9, 1985	51.44	177.91	52	5.6	6.0		ISC

TABLE 1 (continued)

Date	Lat. (°N)	Long. (°E)	Depth (km)	m_b	M_s	F.M.	Ref.
May 9, 1985	51.28	178.03	43	5.4	5.9		ISC
Nov. 2, 1985	51.28	179.27	54	5.1			ISC
Nov. 16, 1985	51.58	177.26	41	5.4	5.0		ISC
June 18, 1986	52.32	179.62	182	5.0			ISC
Dec. 18, 1986	51.68	179.04	76	5.1			ISC

GR49 = Gutenberg and Richter, 1949; FK81 = Fujita and Kanamori, 1981; ISC = Bull. Int. Seismol. Center; HAR = Centroid Moment Tensor solutions from the Harvard Group; WT = Wilson and Toldi, 1978; C = compressional, and S = strike slip focal mechanism.

asperities, obtained by Beck and Christensen (1991) for the 1965 Rat Islands earthquake. The asperity distribution shown in Figure 1 is based on P-wave analysis. The first and largest asperity extends from the epicenter (178.55°E, 51.29°N) to 100 km to the west-northwest and corresponds to a smooth pulse of moment release lasting 50 s. The second pulse of moment release, corresponding to the central asperity, is very jagged and less coherent between stations (Beck and Christensen, 1991) and is centered around 200 km west-northwest of the epicenter. The third pulse of moment release occurs around 420 km west-northwest of the epicenter. Although the aftershocks extend for about 600 km west-northwest of the epicenter, Beck and Christensen (1991) could not resolve any moment release from P-waves beyond the western asperity. It should be mentioned here that the method used in this analysis allows for the placement of seismic moment release pulses (asperities) only along the strike, and the dip positions or extent of particular asperities are not resolvable. We chose to show the asperities obtained by Beck and Christensen (1991) from the P-wave analysis because they agree reasonably well either with the results obtained earlier and with the use of other techniques (Wu and Kanamori, 1973; Mori, 1984; Kikuchi and Fukao, 1987), or with the results of Beck and Christensen (1991) obtained by the tomographic inversion method devised by Ruff (1987) and by multi-station inversion following the technique developed by Kikuchi and Kanamori (1982). Comparisons of spatial and temporal heterogeneities of seismic moment release of the Rat Islands 1965 earthquake obtained by different researchers and/or different methods show that the moment release is concentrated near the epicenter and also around 173°E, with a more dispersed region of moment release near the center of the rupture zone.

For oblique subduction, as is the western Aleutians segment where the Rat Islands 1965 earthquake occurred, it is difficult to formulate the hypothesis about which part of the outer-rise area would be affected most by the high slip on an asperity: should it be the area in front of the asperity, when looking perpendicular to the trench, or should we rather consider the direction of plate motion? In other words: what are the details of relative motion, and hence orientations (relative to the asperity) of regions where stress fluctuations are likely to be most significant in an obliquely subducting segment? Comparison of directions of plate motion and slip vectors for earthquakes located along the interface of the whole Aleutian arc shows only a modest angular discrepancy, increasing towards the west and amounting to 30° around 175°E, with slip vectors being oriented slightly more normal to the trench than are relative plate motions (Ekström and Engdahl, 1989). It is proposed (Ekström and Engdahl, 1989) that a partitioning of slip occurs, with the discrepant portion of the along-arc motion occurring along a weak strike-slip shear zone in the upper plate, near the volcanic line. These observations would suggest that the outer-rise areas affected most by the high slip at asperities would not be located perpendicular to the trench as measured from the asperities but, rather, more in the direction of plate motion from the asperities (though, as observations of Ekström and Eng-

dahl, 1989, suggest, not completely, and this would depend on how oblique the segment is). Also, according to our hypothesis, the intermediate-depth areas in the downgoing slab would be affected most by the high slip at asperities in zones oriented close to the direction of plate motion down-dip from the asperities. Here we will try to check this hypothesis on outer-rise and intermediate-depth seismicity associated with the Rat Islands 1965 event.

Figure 1 presents the epicenters of earthquakes in the outer-rise and pre-trench area adjacent to the main rupture zone; all earthquakes are listed in Table 1. We use the ISC catalogue and cover the period between February 4, 1965 and August 31, 1987. Figure 1a shows all earthquakes with $m_b \geq 5.0$, while Figure 1b shows only the seismicity that occurred in the first year after the main event, and Figure 1c only the largest events, with $m_b \geq 5.7$. We assume that these earthquakes represent the mechanical response of the outer-rise and pre-trench area to the heterogeneous slip, and hence heterogeneous stress alteration during the main event, and we analyze their distribution from that point of view.

The two largest events, which we interpret as the strongest response of the outer-rise to the slip during the 1965 Rat Islands earthquake, are in front, relative to the direction of plate motion, of the strongest, eastern asperity, one of them (March 30, 1965, $M_s = 7.5$) being among the largest extensional outer-rise earthquakes that occurred in this century and the largest of a series of extensional outer-rise events that followed the Feb. 4, 1965 Rat Islands mainshock. The largest event occurred less than two months, and the second large eight months after the mainshock (Table 1).

The occurrence of tensional earthquakes located near the bathymetric trench and following the Feb. 4, 1965 mainshock has been recognized first by Stauder (1968a,b) who suggested that tensional stress has been transmitted to the outer-rise as a result of the slip during the main event. Stauder (1973) also noted a similar occurrence following the great 1960 Chile earthquake.

As shown in Figure 1, there is a discernible cluster of earthquakes in front of the eastern

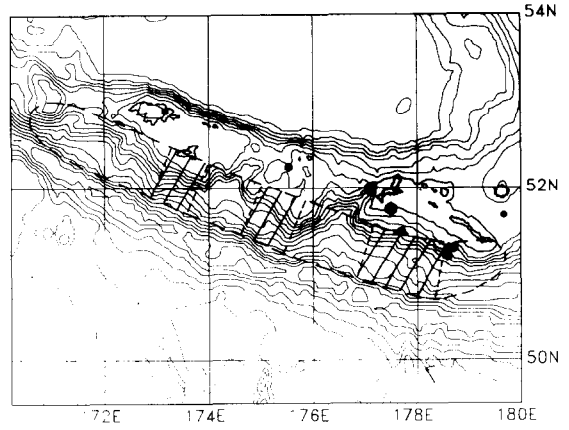

Fig. 2. The aftershock zone (dotted line) of the February 4, 1965 Rat Islands earthquake in the western Aleutians with three areas of highest seismic moment release (hatched, after Beck and Christensen, 1991). Black symbols denote epicenters of earthquakes located at depths more than 40 km, down-dip from the main rupture zone, in the period preceding the mainshock. Size of black symbol is proportional to earthquake magnitude.

asperity, as well as another one in front, again relative to the direction of plate motion, of the western asperity (between 173°E and 174°E), with more diffuse seismicity in the area adjacent to the central part of the main rupture zone (and the central asperity). All larger events (Fig. 1c, $m_b \geq 5.7$) are located adjacent to different asperities, in the direction of incoming plate motion. There are very few or no earthquakes adjacent to the most western and eastern ends of the rupture zone, that is to the areas which did not slip much during the mainshock.

Figure 2 presents the epicenters of earthquakes located down-dip from the main rupture zone in the downgoing slab, at depths between 40 and 250 km. These earthquakes occurred before the main event (the earliest shown occurred in 1940, Table 1) and data quality is poor. Still, it is possible to notice the correlation between the seismic activity in the slab at intermediate depths and the presence of asperities. In particular, the majority of earthquakes occurred approximately down-dip from the strongest, eastern asperity, four of them with $m_b \geq 5.8$, and the largest one, with $m_b = 6.5$, is located straight down-dip from the asperity. The other earthquakes are located

down-dip and in the direction of plate motion from the other two asperities.

Figure 3 presents the epicenters of earthquakes located down-dip from the main rupture zone in the downgoing slab, for a time period between the mainshock and August 31, 1987, data being taken from the ISC catalogues. Figures 3a and 3b show earthquakes with $m_b \geq 5.0$, while Figure 3c shows only the largest of them, with $m_b > 5.7$. We have removed epicenters of earthquakes located in the slab under the main coupled area that ruptured in the mainshock, leaving only the ones under the very edge of the rupture zone and down-dip of it. It is very difficult to assess the position of the lower edge of the main rupture zone, so we are showing here two views of the down-dip seismicity: one for earthquakes deeper than 40 km (Figure 3a), and the other one (Fig. 3b) for earthquakes deeper than 50 km. For Figure 3a we follow the recommendation of Bart Tichelaar (pers. commun., 1991), who searched for the extents and positions of coupled interplate interfaces in different subduction zones, based on mechanisms of earthquakes with $m_b > 6.0$, placing the lower edge of the coupled interface in the western Aleutians at 36–41 km. For Figure 3b we place the lower edge of the rupture zone tentatively at 50 km depth, based on the assumption that in general the down-dip extents of large earthquakes are not well resolved, and that such earthquakes might perhaps overshoot the area marked by after-

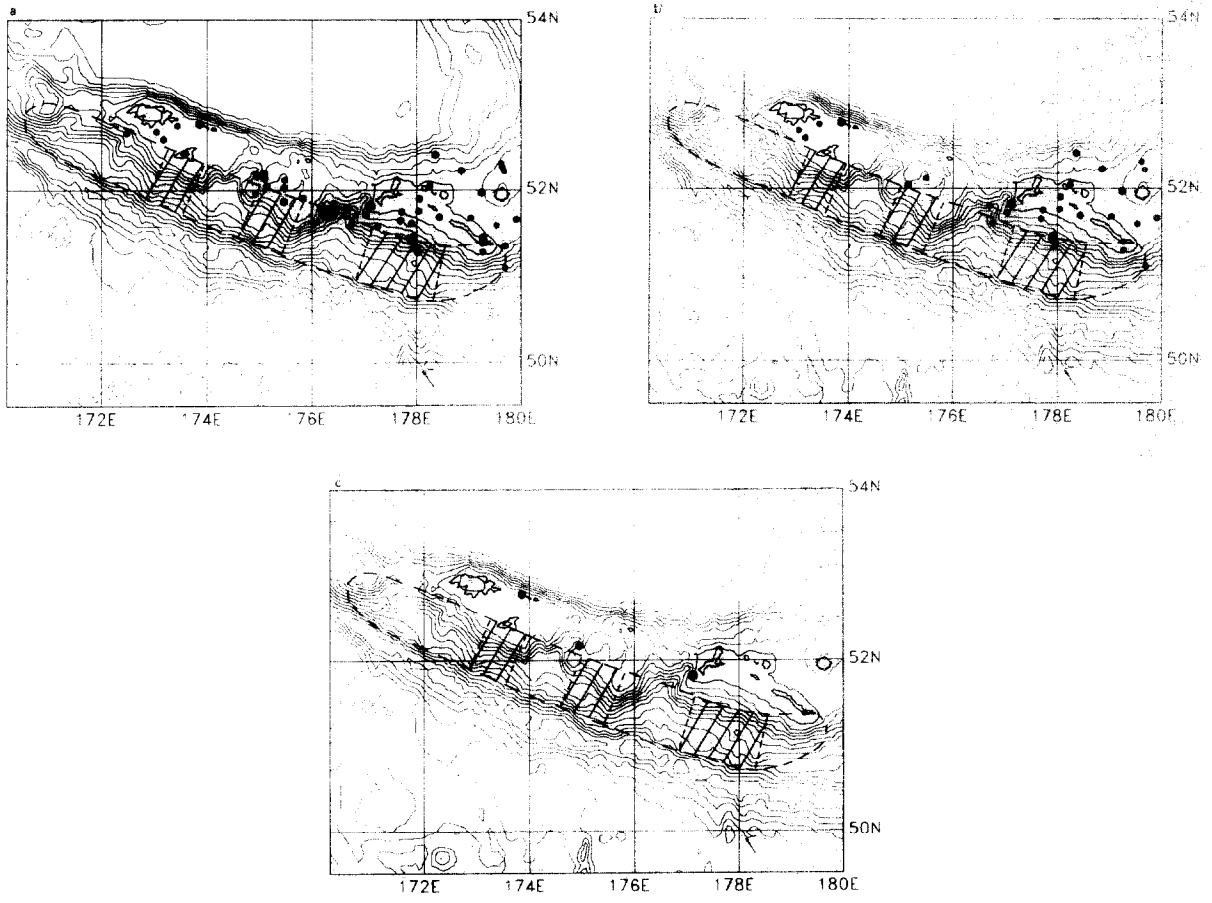

Fig. 3. The aftershock zone (dotted line) of the February 4, 1965 Rat Islands earthquake in the western Aleutians with three areas of highest seismic moment release (hatched, after Beck and Christensen, 1991). Black symbols denote epicenters of earthquakes located down-dip from the main rupture zone, in the downgoing slab, for the time period between Feb. 4, 1965 and Aug. 31, 1987. (a and b) Events with $m_b \geq 5.0$: (a) for depths greater than 40 km; (b) for depths greater than 50 km. (c) The three largest earthquakes that occurred in the downgoing slab following the 1965 Rat Islands event.

shocks. Figures 3a and 3b show that in general, earthquakes in the slab are located down-dip from the areas of highest seismic moment release in the mainshock, the pattern being more clear for the 50 km cut-off depth (Fig. 3b). We do not want to comment on the cluster of earthquakes in Figure 3a around 176.5°E, as they are shallow, with depths between 40 and 50 km, and we are not sure if they belong to the seismicity in the main rupture zone, or they are indeed in the downgoing slab.

Figure 3c shows the three largest earthquakes that occurred in the downgoing slab following the 1965 Rat Islands event. Each of these earthquakes occurred down-dip from one of the asperities, with the biggest one situated down-dip from the strongest, eastern asperity.

In conclusion, in the western Aleutians we observe quite a strong correlation between the distribution of asperities, defined as the areas of highest seismic moment release in the main subduction earthquake, and location of seismic activity both in the outer-rise and at intermediate depths, in the downgoing slab, before and after the mainshock. This is consistent with the notion that such asperities are areas that slip mainly during the mainshock, and are locked at other times, while the other zones slip continuously seismically and/or aseismically, with only a little slip occurring in the mainshock. Thus the significant, seismicity-inducing, changes in stress in the adjacent areas of the ocean floor and slab occur near to those asperities.

As a comment, we note that Beck and Christensen (1991) compared the distribution of their asperities for the 1965 Rat Islands earthquake with aftershocks relocated by Spence (1977), to see if indeed the areas outside the asperities slip more, at least in aftershocks. They observe that there is a lack of aftershocks inside the eastern and western asperities, with some aftershocks located inside the area of the central, possibly less strong asperity.

Also, as the recent work of Geist et al. (1988) shows, the overriding plate along the western Aleutian subduction zone is laterally segmented into a series of rigid tectonic blocks separated by fault-controlled canyons and extensional basins. Beck and Christensen (1991) suggest that the central undeformed parts of the blocks have the strongest coupling with the downgoing plate and hence are the sites of the largest moment release during an underthrusting earthquake. The three asperities determined from the P-waves correspond to the Rat, Buldir and Near tectonic blocks, respectively. Thus, according to Beck and Christensen (1991), the P-wave seismic moment release of the Rat Islands earthquake is controlled by the lateral segmentation of the overriding plate.

Alaska earthquake of March 28, 1964

The great Alaska earthquake of March 28, 1964 ($M_w = 9.2$), the second largest event in recorded history, ruptured a 800-km-long segment of convergent plate boundary between the Pacific and North American plates along the southern margin of mainland Alaska (Fig. 4). To the southwest, the segment abuts on the area that ruptured in 1938 in a $M_w = 8.2$ earthquake. To the east lies the currently mature (see, e.g., Savage and Lisowski, 1986) Yakataga gap, which extends for about 170 km along the coast of southern Alaska between the rupture zones of the 1964 Alaska and 1979 St. Elias earthquake ($M_w = 7.6$) further to the east, and which apparently last ruptured in a sequence of great earthquakes in September 1899.

The average velocity of plate motion in the area of the mainshock is 7.2 cm/yr at 329° (shown as an arrow in Fig. 4), with the component normal to the trench of 6.3 cm/yr (Astiz et al., 1988).

The aftershock zone based on the first ten days of seismic activity with $m_b \geq 5.0$ is shown by dashed lines in Figure 4; the main event started in the northeast, approximately at the down-dip end of the rupture zone, and ruptured southwest with the initial giant pulse of moment release marked as the hatched area in Figure 4. This is the biggest asperity ever retrieved from an inversion of large earthquake, and we cite its extent after Ruff and Kanamori (1983), who estimate its size as 140–200 km.

Ruff and Kanamori (1983) show a second, much smaller pulse of seismic moment release at

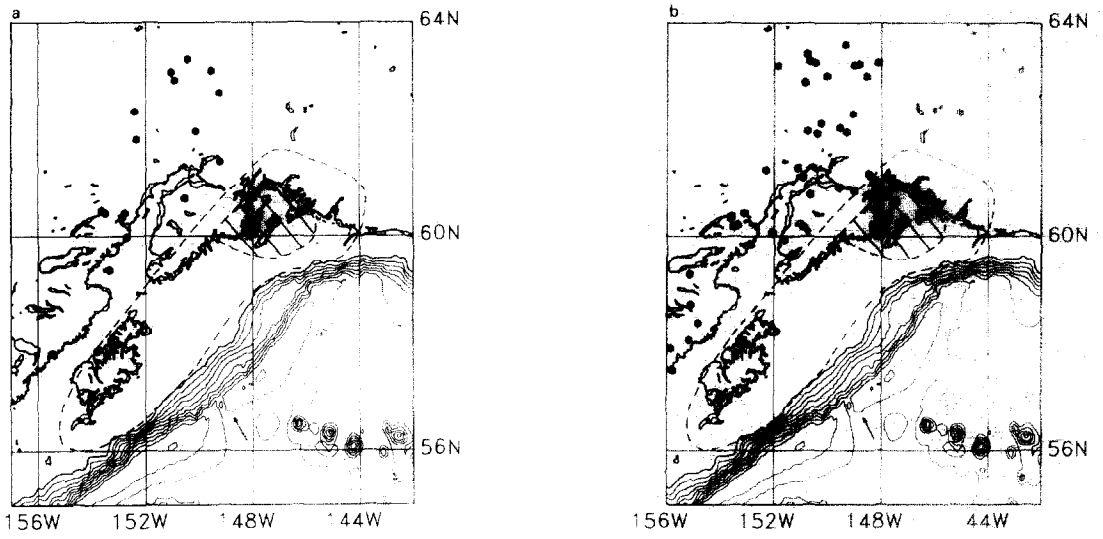

Fig. 4. The aftershock zone (dotted line) of the March 28, 1964 Alaska earthquake, with the highest moment release area after Ruff and Kanamori (1983). Black symbols denote epicenters of earthquakes located at depths more than 70 km down-dip from the main rupture zone, for the time period between Jan. 1, 1954 and March 28, 1964. (a) The most accurately located events; (b) all other (data after Tobin and Sykes, 1966).

around 180 s into the rupture process, though they do not comment on it in their paper. This is what is also calculated, with the use of another inversion technique, by Kikuchi and Fukao (1987), who locate the first area of higher seismic moment release, approximately 200 km in width and 300 km in length, in the eastern end of the rupture zone, and a second, smaller area around 360 to 480 km southwest from the epicenter. Thus, according to Kikuchi and Fukao (1987), the first asperity is even larger than estimated by Ruff and Kanamori (1983), and there is a second, smaller asperity, approximately at the position of Kodiak Island.

Very similar (though still preliminary) results to that obtained by Kikuchi and Fukao (1987) were presented recently by Christensen and Beck (1989), who followed the technique of Ruff and Kanamori (1983) and found two asperities, the first one extending over the northeastern one-third of the aftershock area, and a smaller one, located about 500 ± 100 km southwest of the epicenter. The authors commented that the poor azimuthal coverage inhibited better resolution of this last location.

Comparison of these different views on the spatial and temporal distribution of seismic moment release during the 1964 Alaska earthquake suggests that perhaps the Ruff and Kanamori (1983) asperity shown in Figure 4 should be treated as a conservative estimate of the main area of moment release, and that there was also another asperity, though with smaller moment release, located around Kodiak Island.

Figure 4 shows the epicenters of intermediate-depth earthquakes located in the downgoing slab, at depths larger than 70 km, for the period of January 1, 1954 to March 28, 1964, that is for the last ten years before the mainshock. All data are listed in Table 2. The data have been collected by Tobin and Sykes (1966), and we show their results for the most accurately located earthquakes in Figure 4a (these are their earthquakes denoted by AA, with the depth errors less than 25 km, and with the best azimuthal station coverage), while all other earthquakes, denoted by AB, BA or BB are shown in Figure 4b. Tobin and Sykes (1966) comment that the standard errors in epicentral locations for their events labeled A do not exceed 10 to 20 km, though, since calibrated travel times were not available for this region, epicentral locations may not be as accurate as the standard errors might suggest.

Presumably the earthquakes in Figure 4a are

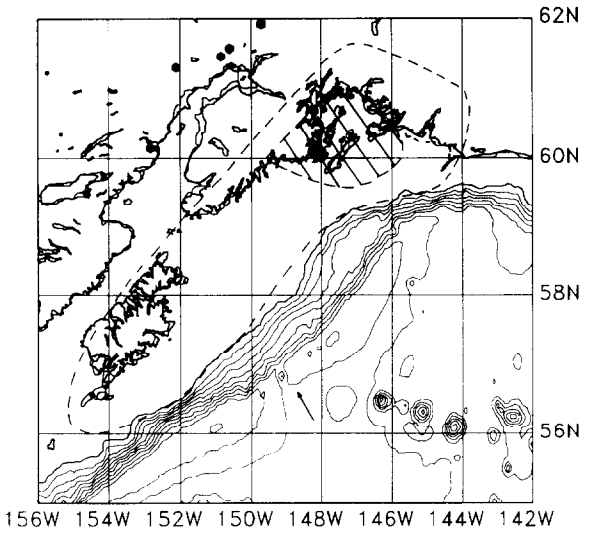

Fig. 5. The aftershock zone (dotted line) of the March 28, 1964 Alaska earthquake, with the highest moment release area after Ruff and Kanamori (1983). Black symbols denote epicenters of earthquakes with $m_b \geq 5.6$ located at depths more than 50 km, down-dip from the main rupture zone, for the period March 28, 1964 to Aug. 31, 1987.

the ones with bigger magnitudes, as they were registered better and at more stations than the others.

We realize that these are old earthquakes, preceding the installation of the WWSSN global seismic network, and that we should not overinterpret their positions or depths. However, even conservative inspection of Figure 4 reveals that the biggest earthquakes that occurred in the downgoing slab at intermediate depths during the last ten years before the mainshock (Fig. 4a) are located mainly down-dip from the area that had the highest seismic moment release during the Alaska 1964 event (that is down-dip from the main asperity).

The epicenters of the largest earthquakes ($m_b \geq 5.6$) located at intermediate depths (more than 50 km) in the downgoing slab, down-dip from the main rupture zone, following the main event for almost 25 years (up to August 31, 1987) are presented in Figure 5. The data are taken from the ISC catalogues and listed in Table 2. Four out of five of these earthquakes are located down-dip from the main asperity.

We chose to show only the largest intermediate-depth events, as we interpret them as indicating these parts of the downgoing slab that have been affected most by the irregular slip in the

TABLE 2

Alaska earthquake of March 28, 1964

Date	Lat. (°N)	Long. (°W)	Depth (km)	m_b	M_s	F.M.	Ref.
(A) Intermediate-depth earthquakes							
Events denoted by AA from Tobin and Sykes, 1966:							
Oct. 3, 1954	60.71	150.52	73				TS
Nov. 25, 1957	62.90	150.90	115				TS
June 4, 1959	59.98	152.70	99				TS
Jan. 16, 1960	63.29	150.41	125				TS
Sept. 12, 1960	60.43	153.50	171				TS
Nov. 2, 1960	57.85	153.81	75				TS
Nov. 27, 1960	63.06	151.03	122				TS
Dec. 21, 1960	61.81	152.35	102				TS
Jan. 12, 1961	57.81	155.47	75				TS
Spet. 25, 1961	60.36	152.88	117				TS
Feb. 27, 1962	63.08	149.53	93				TS
Mar. 21, 1962	62.33	152.40	116				TS
May 10, 1962	61.96	150.11	82				TS
June 18, 1962	60.48	153.64	169				TS
Oct. 21, 1962	61.39	149.21	71				TS
Jan. 27, 1963	59.36	153.34	75				TS
Dec. 14, 1963	62.66	149.22	70				TS
Mar. 8, 1964	60.43	152.77	158				TS

TABLE 2 (continued)

Date	Lat. (°N)	Long. (°W)	Depth (km)	m_b	M_s	F.M.	Ref.
Events denoted by AB, BA, BB from Tobin and Sykes, 1966:							
Jan. 27, 1954	57.49	155.80	73				TS
Apr. 24, 1954	62.99	148.54	90				TS
Aug. 23, 1954	60.92	149.55	84				TS
Oct. 3, 1955	56.32	160.94	164				TS
Nov. 25, 1955	59.29	155.15	95				TS
Nov. 27, 1955	57.91	155.86	79				TS
Dec. 29, 1955	60.34	153.63	109				TS
Mar. 2, 1956	63.57	149.33	79				TS
May 18, 1956	62.32	145.04	103				TS
Nov. 10, 1956	58.72	155.12	131				TS
Apr. 4, 1957	58.06	155.18	74				TS
May 22, 1958	60.79	150.64	156				TS
Feb. 3, 1959	60.07	152.06	111				TS
Mar. 19, 1959	61.29	151.11	108				TS
Dec. 7, 1960	62.99	150.01	79				TS
Jan. 18, 1961	61.97	150.74	108				TS
Jan. 20, 1961	60.21	153.37	146				TS
Sept. 8, 1961	63.24	150.46	133				TS
Sept. 25, 1961	61.25	152.30	80				TS
Dec. 25, 1961	60.86	149.00	71				TS
Jan. 24, 1962	59.94	151.60	114				TS
Apr. 1, 1962	63.40	150.75	141				TS
Apr. 14, 1962	59.67	151.33	81				TS
Sept. 23, 1962	60.18	150.89	84				TS
Nov. 17, 1962	63.27	150.65	119				TS
Dec. 8, 1962	62.87	150.82	90				TS
Dec. 31, 1962	62.29	149.06	83				TS
Jan. 6, 1963	62.88	150.84	128				TS
Jan. 21, 1963	59.82	149.84	128				TS
Jan. 25, 1963	62.03	149.54	111				TS
Apr. 3, 1963	61.18	148.47	101				TS
May 2, 1963	63.19	149.00	82				TS
May 13, 1963	61.12	150.91	93				TS
June 8, 1963	60.38	153.60	172				TS
June 11, 1963	59.86	152.90	71				TS
July 9, 1963	60.44	153.11	132				TS
Aug. 22, 1963	63.21	148.83	101				TS
Sept. 3, 1963	61.92	150.38	116				TS
Sept. 15, 1963	63.18	151.83	122				TS
Sept. 22, 1963	63.24	148.11	112				TS
Sept. 28, 1963	60.18	153.51	101				TS
Nov. 24, 1963	62.11	150.24	101				TS
Jan. 5, 1964	61.95	149.29	72				TS
Jan. 28, 1964	61.09	147.67	157				TS
Feb. 20, 1964	58.38	154.85	77				TS
Events that occurred after March 28, 1964:							
Jan. 6, 1965	61.30	152.10	50	5.7			ISC
Dec. 17, 1968	60.15	152.82	82	6.0			ISC
Dec. 29, 1974	61.57	150.60	65	5.6			ISC
Jan. 1, 1975	61.92	149.72	58	5.9			ISC
Apr. 18, 1987	61.45	150.85	60	5.7		C	ISC/HAR

TABLE 2 (continued)

Date	Lat. (°N)	Long. (°W)	Depth (km)	m_b	M_s	F.M.	Ref.
(B) Outer-rise earthquakes							
Mar. 28, 1964	56.42	152.01	23	6.1			ISC
Mar. 28, 1964	57.46	149.70	30	5.0			ISC
Mar. 28, 1964	56.51	149.90	35	5.0			ISC
Apr. 1, 1964	57.12	150.80	26	5.0			ISC
Apr. 3, 1964	59.60	144.67	10	5.5			ISC
Apr. 4, 1964	59.34	145.24	10	5.1			ISC
Apr. 5, 1964	59.58	144.70	56	5.2			ISC
Apr. 5, 1964	56.69	150.20	17	4.1			ISC
Apr. 7, 1964	55.70	151.83	20	5.5			ISC
Apr. 11, 1964	59.46	144.84	42	5.0			ISC
Apr. 12, 1964	56.56	151.33	28	5.2			ISC
Apr. 13, 1964	59.57	143.10	24	5.0			ISC
Apr. 13, 1964	59.49	142.70	33	5.3			ISC
Apr. 18, 1964	57.36	149.95	10	5.0			ISC
Apr. 24, 1964	59.49	144.45	19	5.1			ISC
May 1, 1964	57.53	149.74	35	5.2			ISC
May 12, 1964	59.46	144.79	33	5.0			ISC
May 17, 1964	59.46	142.62	35	5.3			ISC
Aug. 2, 1964	56.18	149.90	31	5.5		T	ISC/SB
Oct. 17, 1964	59.47	145.60	2	5.1			ISC
Nov. 11, 1964	59.48	144.48	10	5.2			ISC
Apr. 26, 1965	58.78	142.44	37	5.1			ISC
Aug. 11, 1965	59.36	146.08	15	5.3			ISC
Aug. 24, 1965	59.35	145.88	33	5.1			ISC
Sept. 8, 1965	55.71	155.30	24	5.2			ISC
Sept. 18, 1965	59.38	145.18	5	5.2			ISC
Sept. 30, 1965	59.50	143.70	12	5.1			ISC
Jan. 15, 1966	59.46	144.49	33	5.0			ISC
Jan. 22, 1966	56.03	153.78	30	5.6			ISC
July 14, 1966	56.20	149.87	32	5.0			ISC
Oct. 13, 1966	59.47	145.32	20	5.1			ISC
June 11, 1969	59.57	144.71	5	5.2			ISC
June 18, 1969	59.49	144.90	29	5.2			ISC
July 27, 1969	59.42	145.04	60	5.3			ISC
Feb. 23, 1970	55.05	156.86	28	5.1			ISC
Feb. 24, 1970	59.57	143.40	15	5.1			ISC
Apr. 19, 1970	59.60	142.72	20	5.6			ISC
June 22, 1970	55.31	156.39	25	5.5			ISC
June 22, 1970	55.22	156.69	0	5.1			ISC
Jan. 1, 1971	59.62	144.65	18	5.1			ISC
May 25, 1975	57.33	150.18	26	5.6			ISC
Aug. 18, 1975	57.36	150.22	24	5.2			ISC
Oct. 17, 1975	57.39	149.03	31	5.5			ISC
Oct. 20, 1976	56.38	152.64	38	5.0			ISC
Oct. 22, 1976	56.12	153.26	24	5.4			ISC
Jan. 15, 1983	55.92	154.23	0	5.2			ISC
Feb. 13, 1984	55.67	154.43	0	5.1			ISC
Apr. 21, 1985	55.66	154.52	25	5.1			ISC

ISC = Bull. Int. Seismol. Center; HAR = Centroid Moment Tensor solution, Harvard Group; SB = Stauder and Bollinger, 1966; TS = Tobin and Sykes, 1966; C = compr., T = tensional focal mechanism.

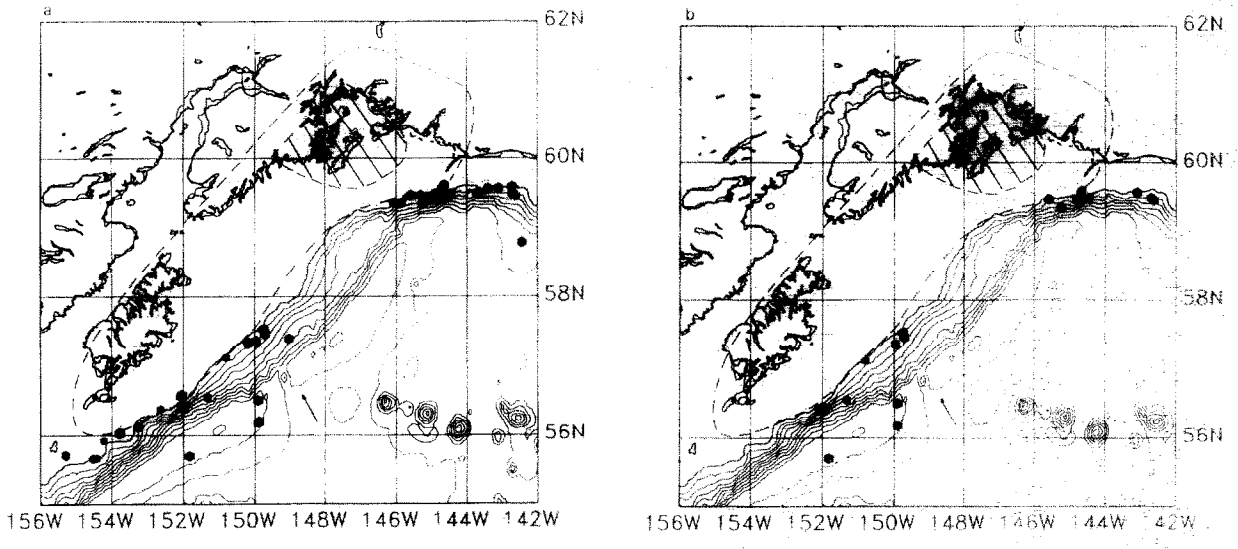

Fig. 6. The aftershock zone (dotted line) of the March 28, 1964 Alaska earthquake, with the highest moment release area after Ruff and Kanamori (1983). Black symbols denote epicenters of earthquakes with $m_b \geq 5.0$ located in trench and outer-rise area for period March 28, 1964 to Aug. 31, 1987. (a) All events, (b) only those which occurred in the first year after the mainshock.

mainshock. These are the same parts that were showing the highest seismicity before the main event (Fig. 4a), resulting from the combined effect of the strongest locking of the main asperity and the sinking of the slab.

Seismic behavior of the pre-trench and outer-rise areas adjacent to the main rupture zone is shown in Figure 6. Figure 6a covers the period following the main earthquake up to August 31, 1987, while Figure 6b shows only the first year following the main event. The data are taken from the ISC catalogues and cover earthquakes with $m_b \geq 5.0$.

There are only two distinct zones of outer-rise events: one adjacent to the main asperity, and the other one, with more diffuse seismicity, adjacent to the second, smaller asperity in the southwestern end of the rupture zone. There is also a clear lack of seismicity, at least at the $m_b \geq 5.0$ level, between these two zones (oceanward from the middle part of the Alaska 1964 rupture zone). We interpret the observed distribution as the response of the outer-rise to the irregular slip in the main event: areas adjacent to zones which slipped more in the main earthquake show some seismicity in the years following the event, while areas adjacent to zones that did not slip much during the main event are quiet.

It is difficult to judge if the earthquakes shown in Figure 6 in the area between 142°W and 144°W are related to the slip in the 1964 Alaska earthquake, or to the slow loading of the currently locked Yakataga gap, or both. That is, it is not clear how far along the strike and/or into the oceanic plate the effects of a large subduction earthquake reach, and only more seismic case studies combined with the results of modeling, e.g., as in Rice and Stuart (1989), could possibly help with finding some answers. Here we only comment that, in the analysis of a series of recent large strike-slip earthquakes that occurred in the northern Gulf of Alaska after the period covered by our Figure 6 (on November 30, 1987, at 58.91°N, 142.76°W, $M_s = 7.6$, and on March 6, 1988 at 57.23°N, 142.78°W, $M_s = 7.6$), Lahr et al. (1988) attribute them to a combination of enhanced tensional stress in the Pacific plate seaward of and following the great Alaska earthquake of 1964, and compressional stress resulting from collision of the Yakutat terrane with North America, suggesting that the influence of an earthquake as large as the Alaska 1964 might be reaching quite far into the oceanic plate.

Valparaiso earthquake of March 3, 1985

The March 3, 1985 Valparaiso earthquake ($M_w = 8.0$) occurred along the central Chile trench in the area recognized as a seismic gap based on historic seismicity (Kelleher, 1972; Mc-

Cann et al., 1979; Nishenko, 1985; the 10-day aftershock zone is shown in Fig. 7). The previous large event in that area occurred on August 16, 1906 ($M_w = 8.2$ to 8.6) and we show its extent in Figure 7. The first event to rerupture part of the 1906 rupture zone was the July 9, 1971 earthquake ($M_w = 7.5$, e.g., Malgrange et al., 1981; Nishenko, 1985; Korrat and Madariaga, 1986; Christensen and Ruff, 1986; aftershock zone shown in Fig. 7), followed by the 1985 Valparaiso earthquake, and leaving still unruptured a small part of the gap, south of the Valparaiso aftershock zone. The earthquakes are the result of the subduction of the Nazca plate under the South American plate, the direction of convergence being about N81°E (shown in Fig. 7) and convergence rate about 9.1 cm/yr.

Seismicity in that area has been extensively studied from many different points of view, including temporal changes in the stress field in the outer-rise area and at intermediate depths in the downgoing slab associated with earthquake cycles (Christensen and Ruff, 1983, 1986; Astiz and Kanamori, 1986; Dmowska et al., 1988; Dmowska and Lovison, 1988; Lay et al., 1989); here we will concentrate only on possible connections between seismicity and the distribution of asperities.

The details of the rupture process of the Valparaiso 1985 event have been studied by different methods, starting with the work of Christensen and Ruff (1986), who found that the highest seismic moment release was located in the middle of the aftershock zone, in the area between the epicenter (33.135°S, 71.871°W) and a line located approximately 75 km south of it. It should be noted here that the method used by Christensen and Ruff (1986) does not allow to place the asperity along the dip of the rupture plane. Choy and Dewey (1988) placed their highest seismic moment release of the Valparaiso mainshock at the same latitude, but at slightly deeper depth. The same is observed by Houston and Kanamori (1990), who followed the technique of Kikuchi and Kanamori (1982) and Kikuchi and Fukao (1987) and produced the most detailed spatial distribution of the seismic moment release of the Valparaiso event. Barrientos (1988) obtained the slip distribution for the Valparaiso earthquake from geodetic data, and it is generally quite similar to the one derived from Houston and Kanamori (1990). Figure 8 shows the slip distribution (slip in meters) on a model fault from Somerville et al. (1991), derived basically from Houston and Kanamori (1990). The model fault shown in Figure 8 occupies only a portion of the aftershock area, the highest slip occurring in its center, with a smaller asperity at the down-dip edge around 34°S. Figure 7 presents the after-

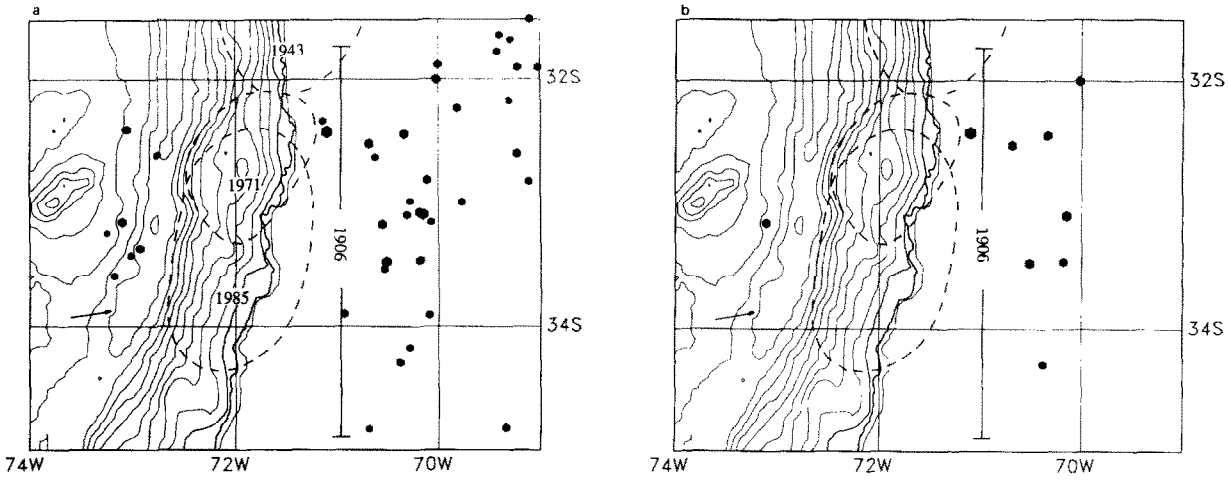

Fig. 7. The aftershock zones (dotted lines) of, from the north, the 1943, 1971 and 1985 earthquakes in central Chile. Black symbols denote epicenters of earthquakes located west of the aftershock zones in the outer-rise area, and east of them, at depths more than 45 km, for the period Jan. 1, 1964 to March 3, 1985. (a) Events with $m_b \geq 5.0$, (b) with $m_b \geq 5.6$.

TABLE 3

Valparaiso earthquake of March 3, 1985

Date	Lat. (°S)	Long. (°W)	Depth (km)	m_b	M_s	F.M.	Ref.
Outer-rise earthquakes:							
Sept. 25, 1971	32.40	73.06	4	5.5		T	ISC/CR
Apr. 16, 1975	33.59	73.18	30	5.1			ISC
July 31, 1980	32.61	72.76	33	5.1			ISC
Oct. 16, 1981	33.15	73.10	18	6.2	7.2	C	ISC/HAR
Oct. 16, 1981	33.36	72.93	33	5.3			ISC
Oct. 22, 1981	33.42	73.02	49	5.1	4.7		ISC
Feb. 25, 1982	33.24	73.25	27	5.0	4.3	C	ISC/KM
Mar. 7, 1985	33.96	72.94	33	4.6			ISC
May 18, 1985	34.31	73.06	33	4.7			ISC
May 18, 1985	34.37	73.21	33	4.6			ISC
July 20, 1985	33.52	72.73	33	4.6			ISC
May 8, 1986	33.22	72.91	28	4.5			ISC
Apr. 18, 1987	33.66	73.08	33	4.8			ISC
June 8, 1990	31.18	73.27	1.0	4.6			PDE
Intermediate-depth earthquakes:							
Sept. 10, 1964	32.99	69.77	95	5.2			ISC
Mar. 28, 1965	32.42	71.10	68	6.4		T	ISC/S73
May 3, 1965	32.44	70.34	81	5.6			ISC
Sept. 26, 1967	33.47	70.51	78	5.7		T	ISC/S73
Mar. 28, 1968	34.82	69.34	164	5.2			ISC
Oct. 13, 1968	32.17	69.31	124	5.0			ISC
Dec. 13, 1969	32.81	70.11	103	5.4			ISC
Apr. 9, 1970	33.91	70.09	120	5.2			ISC
Sept. 17, 1970	31.88	70.00	109	5.3			ISC
Apr. 7, 1971	32.60	69.23	109	5.5			ISC
Sept. 28, 1971	32.00	70.02	104	5.7			ISC
Jan. 13, 1972	32.33	71.14	66	5.1			ISC
Oct. 2, 1972	33.90	70.93	80	5.3			ISC
Jan. 23, 1974	33.23	69.82	103	5.2			ISC
Mar. 24, 1974	33.09	70.31	105	5.2			ISC
Aug. 14, 1974	32.82	69.11	142	5.3			ISC
Nov. 12, 1974	33.17	70.55	86	5.4			ISC
Dec. 29, 1974	33.07	70.19	101	5.3			ISC
Jan. 2, 1975	33.15	70.07	104	5.1			ISC
June 14, 1975	32.52	70.68	92	5.6			ISC
Nov. 17, 1975	31.63	69.40	112	5.2			ISC
Jan. 12, 1977	32.98	70.28	109	5.1			ISC
Aug. 3, 1977	31.67	69.29	51	5.0			ISC
Aug. 29, 1977	31.90	69.22	114	5.3			ISC
Nov. 28, 1977	31.90	69.02	97	5.2			ISC
Jan. 20, 1978	34.29	70.38	112	5.8		T	ISC/HAR
Dec. 30, 1979	32.63	70.62	84	5.1			ISC
July 13, 1980	33.46	70.18	106	5.6	4.4	T	ISC/HAR
Nov. 25, 1980	34.83	70.68	94	5.0			ISC
Dec. 4, 1983	31.77	69.42	113	5.2			ISC
Dec. 15, 1983	33.09	70.15	103	5.9		T	ISC/HAR
May 9, 1984	34.17	70.28	114	5.5		T	ISC/HAR
Oct. 30, 1984	33.53	70.53	92	5.3			ISC
Jan. 31, 1985	31.50	69.10	117	5.2			ISC
Mar. 4, 1985	33.76	71.19	77	5.8		C	ISC/HAR
Mar. 4, 1985	33.13	71.20	72	4.7			ISC

TABLE 3 (continued)

Date	Lat. (°S)	Long. (°W)	Depth (km)	m_b	M_s	F.M.	Ref.
Mar. 29, 1985	34.06	71.32	58	4.7			ISC
Apr. 9, 1985	34.00	71.45	61	6.2		C	ISC/HAR
May 13, 1985	32.78	71.08	68	4.5			ISC
Aug. 24, 1985	33.62	70.14	114	4.5			ISC
Oct. 9, 1985	34.12	71.47	56	5.0			ISC
Nov. 14, 1985	32.42	69.70	114	5.1			ISC
Jan. 5, 1986	32.19	70.82	99	4.8			ISC
June 1, 1986	33.40	70.16	115	4.5			ISC
June 5, 1986	34.43	70.90	91	5.1			ISC
June 17, 1986	31.87	70.09	117	4.9			ISC
July 4, 1986	32.39	70.13	108	4.5			ISC
Sept. 12, 1986	32.34	69.83	116	4.5			ISC
Sept. 21, 1986	31.78	69.72	116	4.5			ISC
Oct. 15, 1986	32.48	69.98	113	4.8			ISC
Oct. 30, 1986	31.68	69.55	130	4.7			ISC
Nov. 23, 1986	32.05	70.31	107	5.0			ISC
Mar. 1, 1987	31.62	69.14	122	4.7			ISC
Mar. 11, 1987	32.05	69.78	104	4.9			ISC
June 27, 1987	32.18	70.11	126	4.8			ISC
Aug. 5, 1987	31.63	69.27	122	4.5			ISC
Nov. 12, 1987	32.09	70.33	118	4.5			PDE
May 30, 1988	31.52	69.06	94	5.8			PDE
June 17, 1988	32.38	69.71	117	4.5			PDE
July 9, 1988	32.37	69.36	121	4.9			PDE
July 12, 1988	32.16	70.70	108	4.7			PDE
Aug. 5, 1988	31.67	69.29	119	4.7			PDE
Jan. 31, 1989	33.96	70.13	127	4.7			PDE
Apr. 1, 1989	32.80	69.95	110	5.5		T	PDE/HAR
July 23, 1989	33.16	70.28	102	4.7			PDE
Nov. 9, 1989	33.91	70.55	96	5.0			PDE

CR = Christensen and Ruff, 1988; ISC = Bull. Int. Seismol. Center; HAR = Centroid Moment Tensor solution of Harvard Group; PDE = preliminary determination of epicenters; S73 = Stauder, 1973; KM = Korrat and Madariaga, 1986; C = compression, S = strike slip; T = tension focal mechanism solutions.

shock zones of the 1971 and 1985 events, with the southern end of the 1943 aftershock zone in the north, and the gap area in the south. Seismicity shown in Figure 7 covers the period between January 1, 1964 and the March 3, 1985 Valparaiso earthquake. All data are taken from the ISC catalogues and listed in Table 3. Shown in Figure 7a are epicenters of earthquakes with $m_b \geqslant 5.0$, west of the aftershock zones in the outer-rise area, and east of them in the downgoing slab, at depths larger than 45 km.

The spatial distribution of seismic moment release in the July 9, 1971 earthquake is not known, but possibly it is concentrated in the northern part of the rupture zone, as the two outer-rise earthquakes that occurred after that event are located in front of its northern part, if we take into account the direction of plate motion. The bigger of the two, a tensional earthquake, occurred on September 25, 1971 ($m_b = 5.5$), clearly in response to the slip in the July 9, 1971 event. We are not aware of any outer-rise earthquakes preceding the July 1971 event, at least at the $m_b \geqslant 5.0$ level.

This is not the case for the Valparaiso 1985 earthquake, which was preceded by a few outer-rise events (a cluster of them shown in Fig. 7a). The largest, shallow compressional event that occurred on October 10, 1981 ($m_b = 6.2$) had been recognized ahead of time as indicating a build-up

of compressional stress in the area of a mature seismic gap (Christensen and Ruff, 1983).

Here we observe, comparing Figures 7 and 8, that the outer-rise earthquakes preceding the Valparaiso event are all located in front of the area of the largest seismic moment release in that earthquake.

Seismicity at the level $m_b \geq 5.0$ in the downgoing slab, preceding the Valparaiso event, shown in the eastern part of Figure 7a, is quite diffuse and does not show any clustering associated with the presence of the asperity. It is perhaps more enlightening to look at the biggest events only, shown in Figure 7b for $m_b \geq 5.6$. We could assume that three large events located at intermediate depths around 32.5°S are all associated with the July 9, 1971 interplate earthquake (aftershock zone shown in Fig. 7b) and loading and unloading of its asperity. The position of that asperity is unknown, but we note that all these earthquakes and the two outer-rise events associated with the 1971 event, and shown in Figure 7a, are conspicuously located in a narrow strip aligned along the direction of plate motion, and are compatible with our tentative assignment of the asperity to the northern part of the 1971 rupture zone as discussed above. Three of the remaining four largest earthquakes located down-dip from the 1985 event are located down-dip from the main asperity of that event in the direction of plate motion.

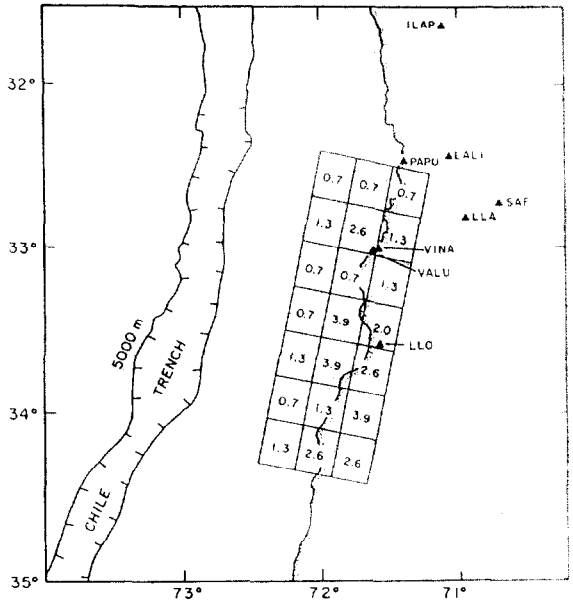

Fig. 8. Map view of the Valparaiso 1985 fault area, with slip in meters in each of the fault elements (after Somerville et al., 1991).

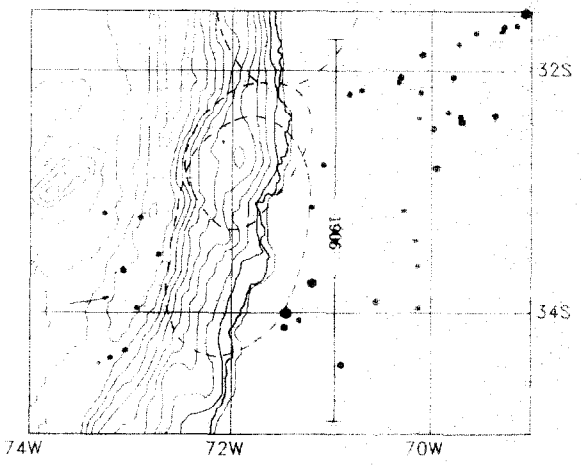

Fig. 9. The aftershock zones (dotted lines) of, from the north, the 1943, 1971 and 1985 earthquakes in central Chile. Black symbols denote epicenters of earthquakes with $m_b \geq 4.5$ located west of the aftershock zones in the outer-rise area, and east of them, at depths more than 45 km, for the period March 3, 1985 to Dec. 31, 1990.

Seismicity after the 1985 Valparaiso earthquake is shown in Figure 9 and listed in Table 3. Both, outer-rise and slab at intermediate depths are very quiet, so Figure 9 shows the epicenters of earthquakes with $m_b \geq 4.5$. The period covered is from the Valparaiso event to August 31, 1987, based on the ISC catalogues, and from September 1, 1987 to December 31, 1990, based on the USGS PDE catalogues. We realize the differences in confidence levels of these two catalogues; however, we would like to inspect as long period of time after the mainshock as possible.

The outer-rise adjacent to the 1985 Valparaiso event did not respond much to the slip that occurred during that earthquake; the biggest event there has $m_b = 4.8$ (April 18, 1987). The outer-rise events are situated in the area that was active before the mainshock, and also spread out towards the south. The only possibly important observation is that the outer-rise adjacent to the northern part of the main rupture (which did slip less in the mainshock) and to the north, along the

trench, is completely quiet for the period shown in Figure 9.

It is interesting to observe that the outer-rise adjacent to the 1985 Valparaiso aftershock area ruptured in (compressional) earthquakes up to $m_b = 6.2$ before the main event, but did not show that much seismicity in the period after the mainshock, while the area just north of it, adjacent to the July 1971 earthquake, did not show any compressional earthquakes before the main event (at least at $m_b \geq 5.0$ level), but responded with a $m_b = 5.5$ earthquake (September 25, 1971) to the slip in the main event.

The slab at intermediate depths down-dip from the aftershock zone of the 1985 Valparaiso event exhibits a lower level of seismicity (at least for the period of almost six years after the main event, covered by Fig. 9) than that before the mainshock (compare Figs. 7 and 9), behavior to be expected (Dmowska et al., 1988) and observed in many other subduction zones (Astiz et al., 1988; Lay et al., 1989). The only two larger events situated down-dip from the mainshock, shown in Figure 9, occurred just after the main event and one of them ($m_b = 6.2$, April 9, 1985) is treated by others as an aftershock (Choy and Dewey, 1988).

Discussion and conclusions

It has been found, based on observations of three cases of large subduction earthquakes with known spatial distributions of seismic moment release, that in general the seismicity in the incoming oceanic plate clusters in front of asperities (= areas of highest seismic moment release and strongest locking). It is usually lacking in areas adjacent to non-asperities, that is to zones that slip during the main event but with appreciably smaller seismic moment release, and possibly slip seismically/aseismically during the whole cycle. Similar behavior occurs in the downgoing slab at intermediate depths, where seismicity during the cycle clusters (but less strongly than in the oceanic crust) next to asperities and down-dip from them.

We infer that the locking of asperities causes higher stress fluctuations associated with the earthquake cycle to occur in areas adjacent to them, both up-dip and down-dip along the direction of plate motion, and that such stressing is much less pronounced in the areas adjacent to non-asperities.

These observations open the possibility of identifying the areas of highest seismic moment release in future large subduction earthquakes along margins for which there is not enough information about the seismic moment release pattern in the past event. Such margins include, e.g., the region that ruptured in the Aleutians 1957 earthquake (and reruptured only in part in the Andreanof Island 1986 event), the zone of the Chile 1960 earthquake, and the Arica (southern Peru) and Antofagasta (northern Chile) segments of the convergent plate margin between the Nazca and South American plates, which ruptured in the August 14, 1868 ($M_t = 9.0$) and May 9, 1877 ($M_t = 9.0$) earthquakes, respectively, and which are capable of producing large tsunamigenic earthquakes. Such results might be also helpful in simulations of the low-frequency component of the strong ground motion spectrum from a future subduction earthquake, for earthquake engineering purposes.

They also carry implications for where the highest deformation, and, possibly, precursory phenomena and/or nucleation of a future event might occur. Further, since strong asperities have different coupling than other areas, the results might have also implications for repeat-time variations along subducting margins.

Acknowledgements

We would like to thank many people who discussed with us over the years the issues of subduction mechanics and asperities in particular. They include Kei Aki, Susan Beck, Doug Christensen, Hiroo Kanamori, Thorne Lay, Jim Rice, Larry Ruff, Bill Stuart and Bart Tichelaar. Also, we are grateful to Adam Dziewonski, Göran Ekström and Wei-jia Su for all discussions and for smoothing our data retrieval efforts. Comments by two anonymous reviewers helped us to improve the text.

The research was supported primarily by the USGS, under grants 14-08-0001-G-1367 and 1788, and in part by NSF under grant EAR-90-04556.

References

Astiz, L. and Kanamori, H., 1986. Interplate coupling and temporal variation of mechanisms of intermediate-depth earthquakes in Chile. Bull. Seismol. Soc. Am., 76: 1614–1622.

Astiz, L., Lay, T. and Kanamori, H., 1988. Large intermediate depth earthquakes and the subduction process. Phys. Earth Planet. Inter., 53: 80–166.

Barrientos, S.E., 1988. Slip distribution of the 1985 central Chile earthquake. Tectonophysics, 145: 225–241.

Beck, S.L. and Christensen, D.H., 1991. Rupture process of the Feb. 4, 1965, Rat Islands earthquake. J. Geophys. Res., 96: 2205–2201.

Beck, S.L. and Ruff, L.J., 1984. The rupture process of the great 1979 Colombia earthquake: Evidence for the asperity model. J. Geophys. Res., 89: 9281–9291.

Beck, S.L. and Ruff, L.J., 1987. Rupture process of the great 1963 Kurile Islands earthquake sequence: Asperity interaction and multiple event rupture. J. Geophys. Res., 92: 14123–14138.

Choy, G.L. and Dewey, J.W., 1988. Rupture process of an extended earthquake sequence: teleseismic analysis of the Chilean earthquake of March 3, 1985. J. Geophys. Res., 93: 1103–1118.

Christensen, D.H. and Beck, S., 1989. Rupture process of the great 1964 Alaska earthquake. EOS, 70: 1225 (abstr.).

Christensen, D.H. and Ruff, L.J., 1983. Outer-rise earthquakes and seismic coupling. Geophys. Res. Lett., 10: 697–700.

Christensen, D.H. and Ruff, L.J., 1986. Rupture process of the March 3, 1985 Chilean earthquake. Geophys. Res. Lett., 13: 721–724.

Christensen, D.H. and Ruff, L.J., 1988. Seismic coupling and outer rise earthquakes. J. Geophys. Res., 93: 13421–13444.

Cormier, V., 1975. Tectonics near the junction of the Aleutian and Kurile–Kamchatka arcs, and a mechanism for middle Tertiary magmatism in the Kamchatka basin. Geol. Soc. Am. Bull., 86: 443–453.

Dmowska, R. and Lovison, L.C., 1988. Intermediate-term seismic precursors for some coupled subduction zones. Pure Appl. Geophys., 126: 643–664.

Dmowska, R., Rice, J.R., Lovison, L.C. and Josell, D., 1988. Stress transfer and seismic phenomena in coupled subduction zones during the earthquake cycle. J. Geophys. Res., 93: 7869–7884.

Ekström, G. and Engdahl, E.R., 1989. Earthquake source parameters and stress distribution in the Adak Island region of the central Aleutian Islands, Alaska. J. Geophys. Res., 94: 15499–15518.

Engdahl, E.R., Billington, S. and Kisslinger, C., 1989. Teleseismically recorded seismicity before and after the May 7, 1986, Andreanof Islands, Alaska, earthquake. J. Geophys. Res., 94: 15481–15498.

Fujita, K. and Kanamori, H., 1981. Double seismic zones and stresses of intermediate depth earthquakes. Geophys. J.R Astron. Soc., 66: 131–156.

Geist, E.L., Childs, J.R. and Scholl, D.W., 1988. The origin of summit basins of the Aleutian Ridge: Implications for block rotation of an arc massif. Tectonics, 7: 327–342.

Hartzell, S. and Iida, M., 1990. Source complexity of the 1987 Whittier Narrows, California, earthquake from the inversion of strong motion records. J. Geophys. Res., 95: 12475–12485.

Houston, H. and Engdahl, E.R., 1989. A comparison of the spatial-temporal distribution of moment release for the 1986 Andreanof Islands earthquake with relocated seismicity. Geophys. Res. Lett., 16: 1421–1424.

Houston, H. and Kanamori, H., 1990. Comparison of strong motion spectra with teleseismic spectra for three magnitude 8 subduction-zone earthquakes. Bull. Seismol. Soc. Am., 80: 913–934.

Kelleher, J.A., 1972. Rupture zones of large South American earthquakes and some predictions. J. Geophys. Res., 77: 2087–2103.

Kikuchi, M. and Fukao, Y., 1985. Iterative deconvolution of complex body waves from great earthquakes—the Tokachi-Oki earthquake of 1968. Phys. Earth Planet. Inter., 37: 235–248.

Kikuchi, M. and Fukao, Y., 1987. Inversion of long period P-waves from great earthquakes along subduction zones. Tectonophysics, 144: 231–247.

Kikuchi, M. and Kanamori, H., 1982. Inversion of complex body waves. Bull. Seismol. Soc. Am., 72: 491–506.

Korrat, I. and Madariaga, R., 1986. Rupture of the Valparaiso (Chile) gap from 1971 to 1985. In: S. Das, J. Boatwright and C.H. Scholz (Editors), Earthquake Source Mechanics. American Geophysical Union, pp. 247–258.

Lahr, J.C., Page, R.A., Stephens, C.D. and Christensen, D.H., 1988. Unusual earthquakes in the Gulf of Alaska and fragmentation of the Pacific plate. Geophys. Res. Lett., 15: 1483–1486.

Lay, T., Astiz, L., Kanamori, H. and Christensen, D.H., 1989. Temporal variation of large interplate earthquakes in coupled subduction zones. Phys. Earth Planet. Inter., 54: 258–312.

Malgrange, M., Deschamps, A. and Madariaga, R., 1981. Thrust and extensional faulting under the Chilean coast: 1965, 1971 Aconcagua earthquakes. Geophys. J.R. Astron. Soc., 66: 313–332.

McCann, W.R., Nishenko, S.P., Sykes, L.R. and Krause, J., 1979. Seismic gaps and plate tectonics: Seismic potential for major boundaries. Pure Appl. Geophys., 117: 1082–1147.

Mendoza, C. and Hartzell, S.H., 1988. Aftershock patterns and mainshock faulting. Bull. Seismol. Soc. Am., 78: 1438–1449.

Minster, J. and Jordan, T., 1978. Present-day plate motions. J. Geophys. Res., 83: 5331–5354.

Mori, J., 1984. Short- and long-period subevents of the 4 February 1965 Rat Islands earthquake. Bull. Seismol. Soc. Am., 74: 1331–1347.

Nishenko, S.P., 1985. Seismic potential for large and great interplate earthquakes along the Chilean and southern Peruvian margins of South America: A quantitative reappraisal. J. Geophys. Res., 90: 3589–3615.

Oppenheimer, D.H., Bakun, W.H. and Lindh, A.G., 1990. Slip partitioning of the Calaveras fault, California, and prospects for future earthquakes. J. Geophys. Res., 95: 8483–8498.

Rice, J.R. and Stuart, W.D., 1989. Stressing in and near a strongly coupled subduction zone during the earthquake cycle. EOS, 70: 1063 (abstr.).

Ruff, L.J., 1983. Fault asperities inferred from seismic body waves. In: H. Kanamori and E. Boschi (Editors), Earthquakes: Observation, Theory and Interpretation. North-Holland, Amsterdam, pp. 251–276.

Ruff, L., 1987. Tomographic imaging of seismic sources. In: G. Nolet (Editor), Seismic Tomography. Reidel, Dordrecht, pp. 339–366.

Ruff, L.J. and Kanamori, H., 1983. The rupture process and asperity distribution of three great earthquakes from long-period diffracted P-waves. Phys. Earth Planet. Inter., 31: 202–230.

Savage, J.C. and Lisowski, M., 1986. Strain accumulation in the Yakataga seismic gap, southern Alaska. J. Geophys. Res., 91: 9495–9506.

Schwartz, S.Y. and Ruff, L.J., 1985. The 1968 Tokachi-Oki and the 1969 Kurile Islands earthquakes: Variability in the rupture process. J. Geophys. Res., 90: 8613–8621.

Schwartz, S.Y. and Ruff, L.J., 1987. Asperity distribution and earthquake occurrence in the southern Kurile Island arc. Phys. Earth Planet. Inter., 49: 54–57.

Schwartz, S.Y., Dewey, J.W. and Lay, T., 1989. Influence of fault plane inhomogeneity on the seismic behavior in the Southern Kurile Islands Arc. J. Geophys. Res., 94: 5637–5649.

Somerville, P., Sen, M. and Cohee, B., 1991. Simulation of strong ground motions recorded during the 1985 Michoacan, Mexico and Valparaiso, Chile earthquakes. Bull. Seismol. Soc. Am., 81: 1–27.

Spence, W., 1977. The Aleutian Arc: Tectonic blocks, episodic subduction, strain diffusion and magma generation. J. Geophys. Res., 82: 213–230.

Stauder, W., 1968a. Mechanism of the Rat Island earthquake sequence of February 4, 1965, with relation to island arcs and sea floor spreading. J. Geophys. Res., 73: 3847–3858.

Stauder, W., 1968b. Tensional character of earthquake foci beneath the Aleutian trench with relation to sea floor spreading. J. Geophys. Res., 73: 7693–7701.

Stauder, W., 1973. Mechanism and spatial distribution of Chilean earthquakes with relation to subduction of the oceanic plate. J. Geophys. Res., 78: 5033–5061.

Stauder, W. and Bollinger, G.A., 1966. The focal mechanism of the Alaska earthquake of March 28, 1964, and of its aftershock sequence. J. Geophys. Res., 71: 5283–5296.

Tobin, D.G. and Sykes, L.R., 1966. Relationship of hypocenters of earthquakes to the geology of Alaska. J. Geophys. Res., 71: 1659–1667.

Wilson, D.S. and Toldi, J.L., 1978. Downdip stresses from deep earthquakes in the Northwestern Pacific. EOS, 59: 1195.

Wu, F.T. and Kanamori, H., 1973. Source mechanism of Feb. 4, 1965, Rat Island earthquake. J. Geophys. Res., 78: 6082–6092.